Calcium Efflux From the Endoplasmic Reticulum Leads to β-Cell Death

Takashi Hara,* Jana Mahadevan,* Kohsuke Kanekura, Mariko Hara, Simin Lu, and Fumihiko Urano

Department of Medicine (T.H., J.M., K.K., M.H., S.L., F.U.), Division of Endocrinology, Metabolism, and Lipid Research, and Department of Pathology and Immunology (F.U.), Washington University School of Medicine, St Louis, Missouri 63110; and Cardiovascular-Metabolics Research Laboratories (T.H.), Daiichi Sankyo Co, Ltd, Tokyo 103-8426, Japan

It has been established that intracellular calcium homeostasis is critical for survival and function of pancreatic β-cells. However, the role of endoplasmic reticulum (ER) calcium homeostasis in β-cell survival and death is not clear. Here we show that ER calcium depletion plays a critical role in β-cell death. Various pathological conditions associated with β-cell death, including ER stress, oxidative stress, palmitate, and chronic high glucose, decreased ER calcium levels and sarcoendoplasmic reticulum Ca^{2+}-ATPase 2b expression, leading to β-cell death. Ectopic expression of mutant insulin and genetic ablation of *WFS1*, a causative gene for Wolfram syndrome, also decreased ER calcium levels and induced β-cell death. Hyperactivation of calpain-2, a calcium-dependent proapoptotic protease, was detected in β-cells undergoing ER calcium depletion. Ectopic expression of sarcoendoplasmic reticulum Ca^{2+}-ATPase 2b, as well as pioglitazone and rapamycin treatment, could prevent calcium efflux from the ER and mitigate β-cell death under various stress conditions. Our results reveal a critical role of ER calcium depletion in β-cell death and indicate that identification of pathways and chemical compounds restoring ER calcium levels will lead to novel therapeutic modalities and pharmacological interventions for type 1 and type 2 diabetes and other ER-related diseases including Wolfram syndrome. **(*Endocrinology* 155: 758–768, 2014)**

Calcium (Ca^{2+}) is involved in diverse physiological processes including muscle contraction, insulin secretion, neurotransmitter release, blood clotting, bone mineralization, and signal transduction (1). Endoplasmic reticulum (ER) stores and pumps Ca^{2+} and serves as the major source of Ca^{2+} for signal transduction (1, 2). Ca^{2+} homeostasis in the ER is maintained by the sarcoendoplasmic reticulum Ca^{2+}-ATPase (SERCA) family of proteins, Ca^{2+} ATPases that pump Ca^{2+} into the ER, and the gated Ca^{2+} channels, inositol triphosphate (IP3) receptors and ryanodine receptors that release Ca^{2+} from the ER (3, 4). Although the loss of Ca^{2+} in the ER has been proposed to play a role in disease states (2, 5, 6), its role in β-cell death in diabetes is still not clear.

Increasing evidence indicates that ER malfunction plays a critical role in β-cell death in type 1 and type 2 diabetes as well as in genetic forms of diabetes including Wolfram syndrome. It has been proposed that ER dysfunction in β-cells triggers autoimmunity during the onset and progression of type 1 diabetes (7, 8). In addition, a number of cytokines have been shown to be important for the development of type 1 diabetes at the level of the ER in β-cells (5, 9, 10). Development of type 2 diabetes mellitus has long been linked to increased body mass index (BMI) and obesity. In accordance with this, recent evidence has shown that circulating free fatty acids (FFA), in particular longer-chain saturated FFAs such as palmitate, causes ER dysfunction in pancreatic β-cells (11–13). ER

ISSN Print 0013-7227 ISSN Online 1945-7170
Printed in U.S.A.

Received June 3, 2013. Accepted November 27, 2013.
First Published Online December 20, 2013

* T.H. and J.M. contributed equally to this work.

Abbreviations: BiP, immunoglobin heavy-chain-binding protein; BMI, body mass index; $[Ca^{2+}]_{cyt}$, cytoplasmic calcium level; $[Ca^{2+}]_{er}$, ER calcium levels; CFP, cyan fluorescent protein; CHOP, CCAAT/enhancer-binding protein homologous protein; ER, endoplasmic reticulum; FACS, fluorescence-activated cell sorting; FBS, fetal bovine serum; FFA, free fatty acid; FRET, fluorescence resonance energy transfer; GAPDH, glyceraldehyde-3-phosphate dehydrogenase; HEK, human embryonic kidney; IAPP, islet amyloid polypeptide; IFN-γ, interferon-γ; INS A24D, insulin A24D; IP3, inositol triphosphate; MIDY, mutant *INS*-gene-induced diabetes of youth; SERCA, sarcoendoplasmic reticulum Ca^{2+}-ATPase; shRNA, short hairpin RNA; TUDCA, tauroursodeoxycholic acid; WFS1, Wolfram syndrome 1; YFP, yellow fluorescent protein.

dysfunction has been shown to play important roles in genetic forms of diabetes including Wolfram syndrome and permanent neonatal diabetes. Juvenile-onset diabetes mellitus and optical atrophy are the characteristic clinical manifestations of Wolfram syndrome (14). In this condition, pancreatic β-cells are selectively destroyed as a consequence of mutations in the *WFS1* gene, which encodes an ER transmembrane protein (15). It has been shown that *WFS1* mutations can cause dysregulation of ER homeostasis (16, 17). ER dysfunction is also involved in β-cell death in patients with permanent neonatal diabetes who have mutations in the preproinsulin (*INS*) gene (18, 19). A number of new preproinsulin gene mutations associated with monogenic diabetes have been discovered and termed mutant *INS*-gene-induced diabetes of youth (MIDY) (18–20). It has been shown that expression of MIDY mutations causes ER dysfunction (21).

These findings prompted us to test the possibility that ER is at the intersection of calcium homeostasis and β-cell death. Here we show that regulation of calcium efflux from the ER plays a critical role in β-cell survival and death.

Materials and Methods

Reagents

Glucose, 2-deoxy-glucose, palmitic acid, oleic acid, dithiothreitol, H_2O_2, thapsigargin, tauroursodeoxycholic acid (TUDCA), cycloheximide, and pioglitazone were obtained from Sigma. Salubrinal was obtained from Calbiochem (EMD Biosciences). Fluo-4 calcium indicator and propidium iodide were obtained from Invitrogen. A caspase3/7 detection kit and a dual-luciferase assay kit were purchased from Promega. Anti-SERCA2b antibody, antispectrin antibody, antiglyceraldehyde-3-phosphate dehydrogenase (GAPDH) antibody, and anti-Wolfram syndrome 1 (WFS1) antibody were purchased from Santa Cruz Biotechnology, Millipore, Cell Signaling Technology, and Proteintech, respectively. Human islet amyloid polypeptide (IAPP) and mouse IAPP were purchased from Bachem.

Plasmids

Calcium-sensing cameleon D1ER was generously gifted from Dr Amy Palmer (University of Colorado, Boulder, Colorado) and the pcDNA3.1 plasmid containing human SERCA2b was gifted from Dr Jonathan Lytton (University of Calgary, Calgary, Canada). Human insulin gene was amplified from pancreas mRNA and A24D mutation was generated by a mutagenesis kit from TOYOBO Biochemicals. WFS1 and the mutants were also constructed by the same methods.

Cell culture

INS-1 832/13 cells were cultured in the RPMI 1640 containing 10% fetal bovine serum (FBS), penicillin and streptomycin, sodium pyruvate and β-mercaptoethanol. Human embryonic kidney (HEK)-293 cells were cultured in DMEM containing 10% FBS and penicillin and streptomycin. Primary humans islets obtained from Prodo were plated onto a six-well plate precoated with laminin V produced by 804G cells and cultured in CMRL medium supplemented with FBS, nonessential amino acids, sodium pyruvate, and antibiotics. For transient transfection, Lipofectamine 2000 (Invitrogen) was used according to the manufacturer's protocol. For establishing stable cell lines, cells were transduced with lentivirus and selected either by puromycin or cell sorting by a fluorescent marker.

Primary islets

Pancreatic islets from db/db mice (7 wk old, male) were isolated by pancreatic duct injection of 1000 U/mL of collagenase solution followed by digestion at 37°C for 15 minutes with mild shaking. Islets were washed several times with Hanks' balanced salt solution, separated from acinar cells on a discontinuous Ficoll 400 gradient, viewed under a dissecting microscope, and hand selected. Human islets from diabetic and control subjects were obtained from Prodo Laboratories.

Preparation of fatty acids

Palmitate and oleate were conjugated with BSA by soaping each fatty acid to sodium hydroxide and mixing with BSA. A 20-mM solution of each fatty acid in 0.01 M NaOH was incubated at 70°C for 30 minutes and then mixed with 5% BSA in PBS in a 1:3 volume ratio. Each solution was diluted with 10% FBS-RPMI 1640 medium to the designated concentration.

Fluorescence-activated cell sorting (FACS) analyses

For flow cytometry analyses, INS-1 832/13 or HEK293 expressing D1ER cameleon were plated onto 12-well plates, treated with each compound for the indicated times, and then harvested by trypsinization. After washing with PBS, cells were resuspended in the Hanks' buffered salt solution. Flow cytometry analyses were performed with LSRII (BD) at the FACS core facility of Washington University School of Medicine. For measuring dead cells, propidium iodide (Invitrogen) was used according to manufacturer's protocols. The results were analyzed by FlowJo version 7.6.3 (Tree Star).

Quantitative real-time PCR

Total RNA was extracted by RNeasy kits (QIAGEN). RT-PCR was performed using ImPromII (Promega) reverse transcriptase, and quantitative PCR was performed with Bio-Rad Laboratories iQ5 using SYBR green dye.

Plate reader

The fluorescence resonance energy transfer (FRET) ratio of the calcium sensor measured by the excitation spectra 434 nm and emission spectra 530 nm/477 nm were determined by Inifinite M1000 (Tecan). INS-1 832/13 cells were plated onto a 96-well plate at 100 000 cells/well and pretreated with various compounds or treated together with thapsigargin, and then the fluorescence was measured after 5 hours.

Statistical analyses

Percentage of positive cells (y) was measured as a proportion of positive cells among all green fluorescent protein-positive cells treated. Frequently arcsine $[\sqrt{(y)}]$ transformation is applied to

the raw data to homogenize the variance before further data analysis. Therefore, all the analyses for percentage of positive cells were performed on transformed data. A set of predetermined contrasts were performed in the framework of one-way ANOVA in R.

Results

To monitor ER calcium levels ($[Ca^{2+}]_{er}$) in cells, we used ER-localized calcium sensor, D1ER, containing a calcium-binding calmodulin domain between two fluorescent proteins, cyan fluorescent protein (CFP) and yellow fluorescent protein (YFP) (22). The calmodulin domain binds Ca^{2+} and brings CFP and YFP into close proximity, which results in the FRET from the CFP to the YFP (Figure 1A). The FRET signal allows ratiometric measurements of free $[Ca^{2+}]_{er}$ and the changes in $[Ca^{2+}]_{er}$ using FRET to CFP ratio. To test whether this system works in the pancreatic β-cell line, the FRET to CFP ratio was measured in INS-1 832/13 cells stably expressing D1ER by FACS. We confirmed that D1ER was localized to the ER (Figure 1B). The treatment of these cells with EGTA, a Ca^{2+} chelating agent, after the membrane permeabilization by digitonin caused the minimum value of the FRET to CFP ratio, whereas $CaCl_2$ treatment together with digitonin led to the maximum value of FRET to CFP ratio (Figure 1C). We categorized cells that had a FRET to CFP ratio lower than 0.8 as ER calcium-depleted cells. The FRET to CFP ratio was decreased in INS-1 832/13 cells by thapsigargin, an inhibitor for SERCA in a dose-dependent manner (Figure 1D). Rates of ER calcium-depleted cells increased in INS-1 832/13 cells by thapsigargin treatment in a dose-dependent manner (Figure 1E). Thapsigargin treatment also induced cell death in a dose-dependent manner (Figure 1F).

To study the relationship between ER calcium depletion, ER stress, and cell death, we measured expression levels of two ER stress markers, CCAAT/enhancer-binding protein homologous protein (CHOP) and immunoglobin heavy-chain-binding protein (BiP), in these cells. Expression levels of CHOP and BiP significantly increased with 30 nM thapsigargin (Figure 1, G and H), which was consistent with the strong induction of cell death (Figure 1F). These results suggest that there is a threshold of ER calcium concentration that leads to ER stress-mediated cell death. We also monitored ER calcium levels in INS-1 832/13 cells at multiple time points and confirmed that these cells were not undergoing ER calcium fluctuations (Figure 1G). Collectively these results indicate that the FRET to CFP ratio can be used for real-time live monitoring of $[Ca^{2+}]_{er}$ of β-cells.

High circulating glucose and FFAs play a role in β-cell dysfunction and death during the progression of diabetes (23). Therefore, we studied the effects of chronic high glucose and FFAs on $[Ca^{2+}]_{er}$ in β-cells using the ER calcium sensor. As expected, the rate of ER calcium-depleted cells was increased by chronic high glucose in a time-dependent manner in INS-1 832/13 cells stably expressing D1ER (Figure 2, A and B). Chronic high glucose treatment also induced caspase-3/7 activation, reflecting cell death (Figure 2C). It has been shown that glucose metabolism plays a role in β-cell dysfunction mediated by chronic high glucose, raising the possibility that inhibition of glucose metabolism could prevent the decrease in $[Ca^{2+}]_{er}$. As we predicted, treatment of INS-1 832/13 cells by chronic high glucose together with 2-deoxyglucose, an inhibitor of glucose metabolism, could block the ER calcium depletion (Figure 2D). Palmitate treatment also increased the rate of ER calcium-depleted INS-1 832/13 cells in a time-dependent manner (Figure 2E). It has been established that high glucose exacerbates palmitate-induced β-cell dysfunction (24–27), which prompted us to measure $[Ca^{2+}]_{er}$ in INS-1 832/13 cells treated with palmitate and high glucose. As expected, high glucose enhanced ER calcium depletion mediated by palmitate (Figure 2F), leading to an increase in cytoplasmic calcium levels ($[Ca^{2+}]_{cyt}$) (Figure 2G). In contrast, oleic acid, which has been shown to be protective against palmitate-induced β-cell dysfunction (25), significantly decreased the rate of ER calcium-depleted cells and suppressed cell death induced by palmitate (Figure 2, F and H). The baseline $[Ca^{2+}]_{cyt}$ was higher in the cells treated with palmitate and palmitate + high glucose than in untreated cells, indicating that palmitate and palmitate + high glucose induce efflux of ER calcium (Figure 2G). Other β-cell stressors such as human islet amyloid polypeptide (Figure 2I), ER stress inducer dithiothreitol (Figure 2J), oxidative stress inducer hydrogen peroxide (Figure 2J), and a cocktail of cytokines consisting of IL-1β, TNFα, and interferon-γ (IFN-γ) (Figure 2K) also increased the rates of ER calcium-depleted cells. Collectively these results indicate that agents perturbing β-cell function generally decrease $[Ca^{2+}]_{er}$.

Next we tested whether genetic factors inducing β-cell death could decrease ER $[Ca^{2+}]_{er}$. Insulin A24D (INS A24D) mutation is known to cause β-cell death in some patients with MIDY (28). The A24D mutation is located at the signal sequence cleavage site of human insulin, shows impaired cleavage of signal peptide, and is retained in the ER (29) (Figure 3A), raising the possibility that expression mutant INS A24D decreases $[Ca^{2+}]_{er}$. Protein expression of proinsulin produced from INS A24D mutant looked higher than that of wild-type because the A24D mutant could not be efficiently processed and accumulated in β-cells (Figure 3B, left bottom panel). We confirmed that mRNA expression of

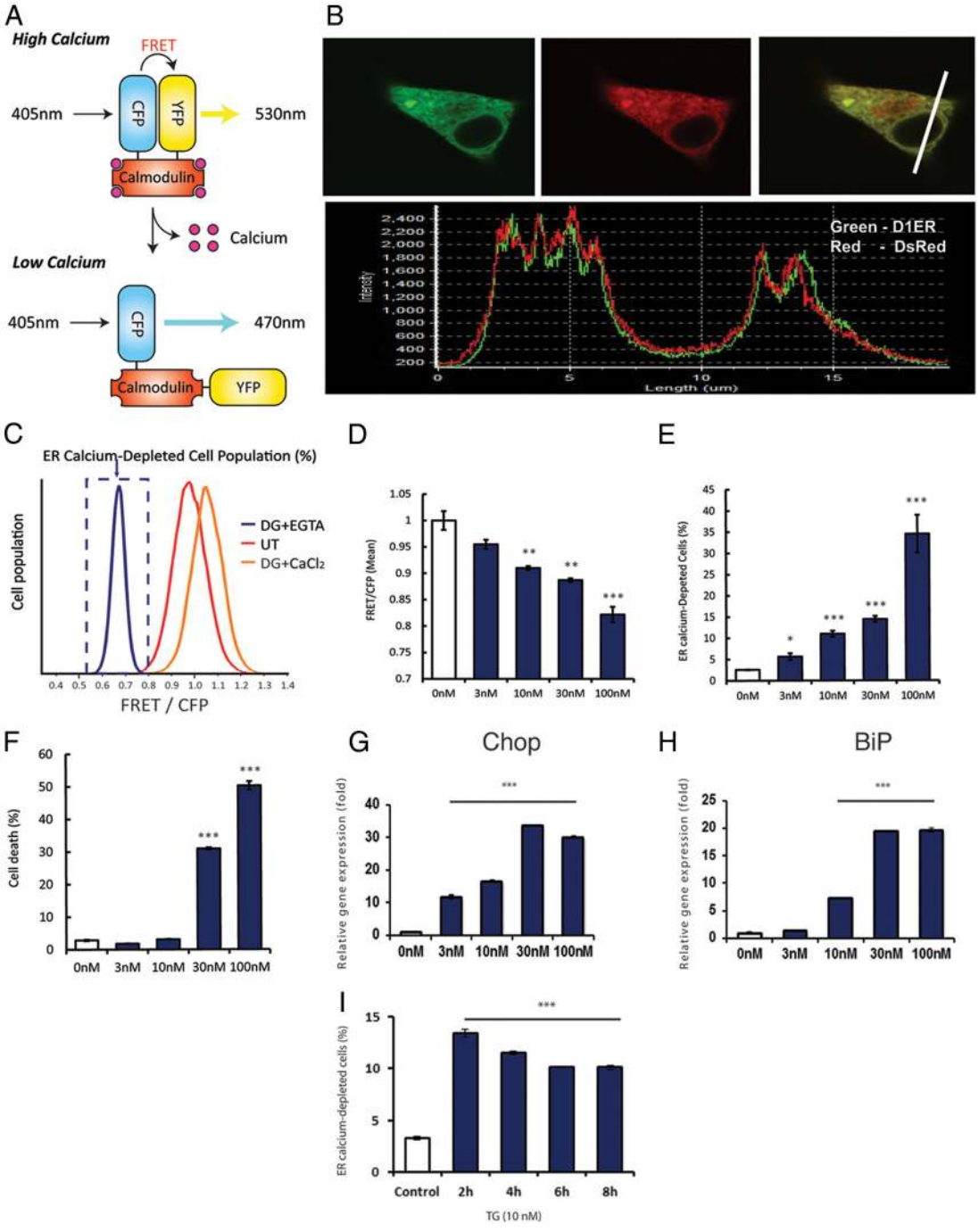

Figure 1. ER calcium sensor monitors ER calcium depletion induced by thpasigargin. A, A schematic representation of the ER calcium sensor (D1ER). The CFP and venus units of calcium sensor are connected by a calcium-sensitive domain consisting of modified calmodulin. Under high-calcium condition, upon binding calcium the calcium-sensitive domain undergoes a conformational change that brings the fluorescent protein domains into close proximity. The resulting FRET signal allows ratiometric measurements of free ER luminal calcium. Under low-calcium condition, calcium dissociates from calcium-sensitive domain and reduces the FRET signal. B, Confocal imaging of INS-1 832/13 cells stably expressing D1ER (left upper panel). ER was visualized by DsRed-ER tracker (Life Technologies) (middle upper panel). A merged image is shown in the right upper panel. The colocalization fluorescence intensity of both D1ER and DsRed are shown (right upper panel). Representative line scans show the fluorescence intensity of D1ER and DsRed-ER tracker. C, FACS analysis of INS-1 832/13 cells stably expressing D1ER untreated, treated with 4 mM EGTA together with 25 μM digitonin (DG), or treated with 10 mM $CaCl_2$ together with 25 μM DG. The x-axis indicates the FRET to CFP ratio and the y-axis indicates the cell population. We categorized cells that had a FRET to CFP ratio lower than 0.8 as ER calcium-depleted cells (n = 3); values are mean ± SEM. *, $P < .05$; **, $P < .01$; ***, $P < .001$. D–F, FACS analysis of INS1 832/13 cells expressing D1ER treated with various concentrations of thapsigargin for 24 hours. The FRET to CFP ratio (D), the rates of ER calcium-depleted cells (E), and the rates of cell death measured by CytoTox-Fluor (Promega) (F) are shown (n = 3); values are mean ± SEM. *, $P < .05$; **, $P < .01$; ***, $P < .001$. G and H, Expression levels of CHOP (G) and BiP (H) mRNA in INS-1 832/13 cells stably expressing D1ER treated with various concentrations of thapsigargin (TG) for 24 hours (n = 3); values are mean ± SEM. ***, $P < .001$. I, FACS analysis of INS-1 832/13 cells stably expressing D1ER treated with 10 nM thapsigargin (TG) for 2, 4, 6, and 8 hours. The rates of ER calcium-depleted cells are shown (n = 3); values are mean ± SE. ***, $P < .001$.

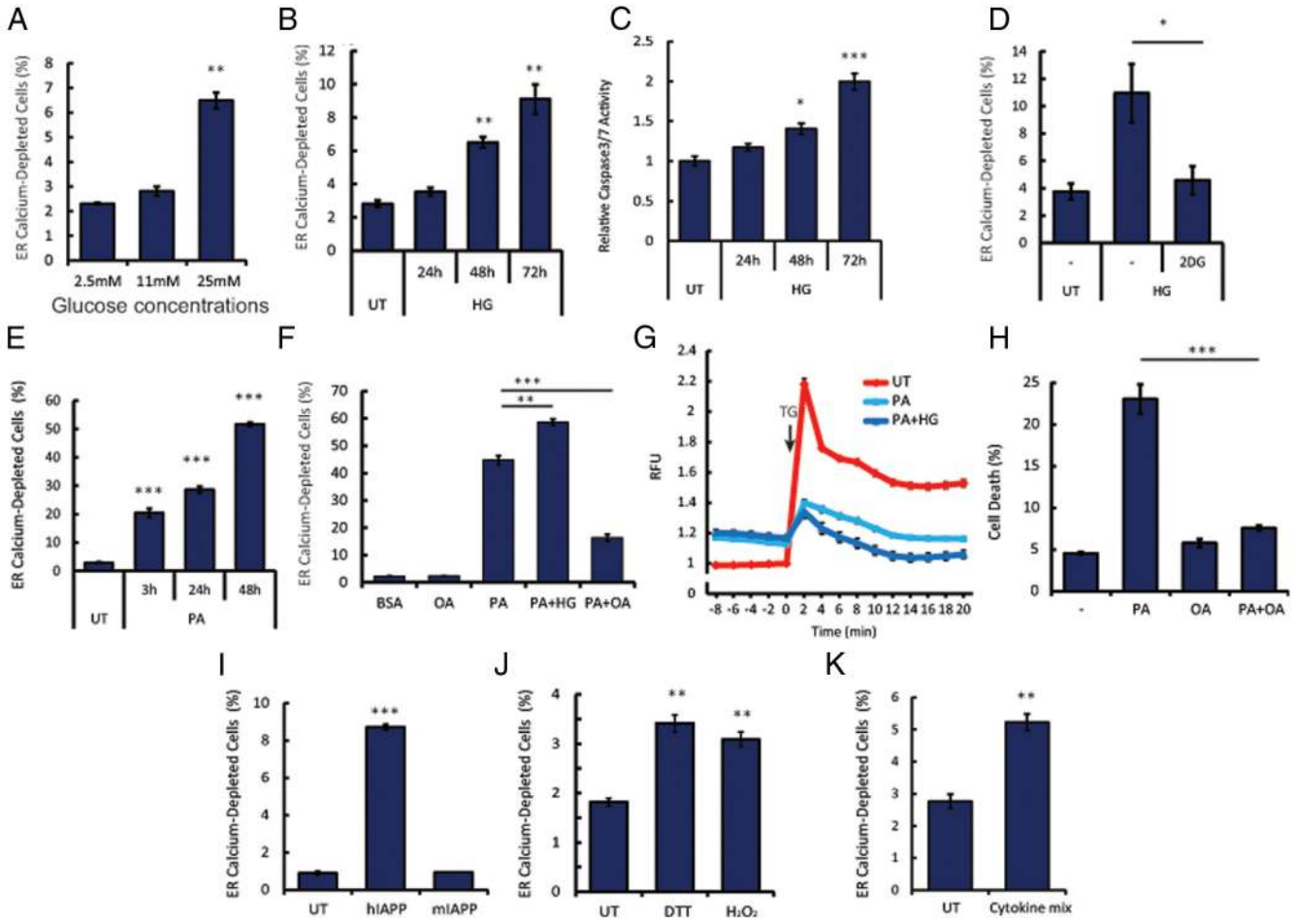

Figure 2. β-Cell stressors induce ER calcium depletion. A, Rates of ER calcium-depleted INS-1 832/13 cells treated with indicated concentrations of glucose for 48 hours. B and C, Rates of ER calcium-depleted cells (B) and cell death (C) in INS-1 832/13 cells treated with 25 mM glucose (HG) for the indicated periods of time. D, Rates of ER calcium-depleted cells in INS1 832/13 treated with or without 25 mM 2-deoxyglucose (2DG) together with 25 mM high glucose (HG) for 48 hours. E, Rates of ER calcium-depleted INS-1 832/13 cells untreated or treated with 0.5 mM palmitic acid for the indicated periods of time. F, Rates of ER calcium-depleted INS-1 832/13 cells untreated (BSA) or treated with 0.5 mM oleic acid (OA), 0.5 mM palmitic acid (PA), 0.5 mM palmitic acid combined with high glucose (PA+HG), or 0.5 mM palmitic acid combined with 0.5 mM oleic acid (PA+OA) for 24 hours. G, Cytosolic calcium levels in INS1 832/13 cells untreated (UT) or treated with 0.5 mM palmitic acid (PA) or 0.5 mM palmitic acid together with high glucose (PA+HG) for 24 hours. The calcium efflux from the ER was induced by 3 μM thapsigargin at time 0 (arrow), and the calcium level was determined by Fluo-4 staining. H, Rates of cell death in INS-1 832/13 cells untreated (UT) or treated with 0.5 mM palmitic acid (PA), 0.5 mM oleic acid (OA), or both (PA+OA) were determined by propidium iodide staining. I, Rates of ER calcium-depleted INS-1 832/13 cells untreated (UT) or treated with freshly dissolved 10 μM human IAPP (hIAPP) or mouse IAPP (mIAPP) for 24 hours. J, Rates of ER calcium-depleted INS1 832/13 cells untreated (UT) or treated with 1 mM dithiothreitol or 1 mM H_2O_2 for 1 hour. K, Rates of ER calcium-depleted INS-1 GC cells untreated or treated with cytokines (100 ng/mL IL1-β, 100 ng/mL TNFα, and 100 ng/mL IFN-γ) for 24 hours. All values are means ± SEM (n = 3). *, $P < .05$; **, $P < .01$; ***, $P < .001$.

INS A24D was comparable with that of wild-type (Figure 3B, right panel). Ectopic expression of INS A24D in INS-1 832/13 cells significantly increased the rate of ER calcium-depleted cells and cell death (Figure 3B, left upper panel, and Figure 3, C and D). The rates of ER calcium-depleted cells were increased by ectopic expression of INS A24D in a dose-dependent manner (Figure 3C). We therefore considered the possibility that decrement of ER-retained INS A24D could prevent the decrease in $[Ca^{2+}]_{er}$. To test this idea, we treated INS-1 cells expressing INS A24D with chemical compounds that could potentially reduce ER-retained INS A24D. As we predicted, treatment of these cells with a chemical chaperone, TUDCA, as well as translation inhibitors, cycloheximide and salubrinal, prevented ER calcium depletion and cell death in INS-1 832/13 cells expressing INS A24D (Figure 3E).

Loss of function of the *WFS1* gene causes β-cell death in Wolfram syndrome, an autosomal recessive disorder characterized by juvenile-onset diabetes and early-onset neurodegeneration (15). It has been shown that β-cell death in Wolfram syndrome is associated with ER stress (16, 17, 30–32), raising the possibility that loss of function of the *WFS1* gene leads to ER calcium depletion. RNA

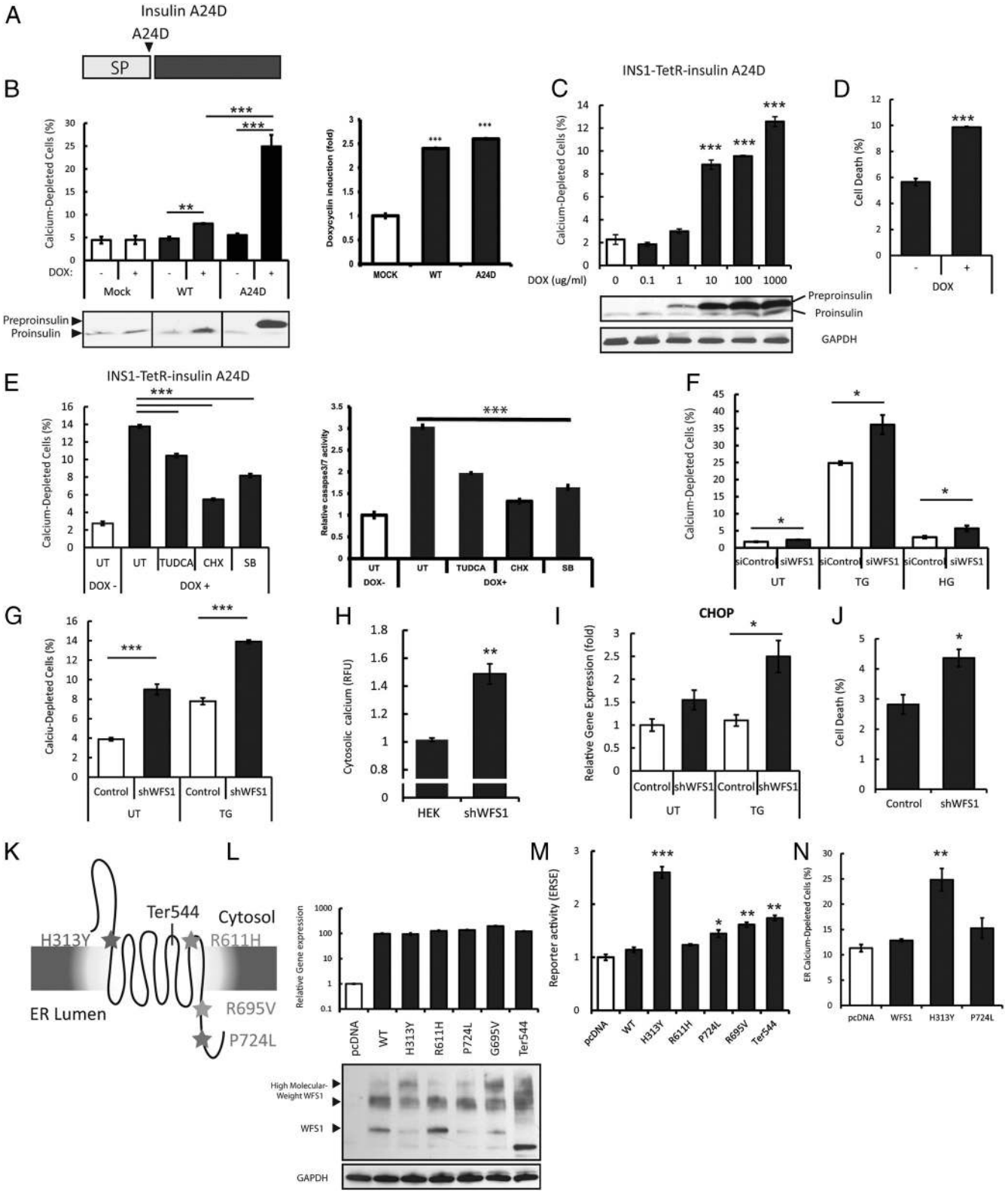

Figure 3. Genetic factors involved in β-cell death induce ER calcium depletion. A, Schematic structure of A24D mutant preproinsulin. SP, signal peptide. B, Rates of ER calcium-depleted INS-1 832/13 cells and INS-1 832/13 cells ectopically expressing wild-type (WT) or mutant A24D (A24D) preproinsulin by a doxycycline (DOX)-inducible system (2 μg/mL of DOX for 48 hours) (left, upper panel). Protein expression levels of endogenous and ectopically expressed wild-type or mutant preproinsulin and proinsulin are shown (left, lower panel). Expression levels of WT or A24D preproinsulin mRNA levels after the DOX treatment (right panel). C, Rates of calcium-depleted INS-1 832/13 cells expressing different amounts of mutant A24D preproinsulin induced by indicated concentrations of doxycycline (DOX). Protein expression levels of preproinsulin and proinsulin, and GAPDH are shown in the middle and bottom panels, respectively. D, Rates of cell death in INS-1 832/13 cells ectopically expressing A24D

interference-mediated knockdown of WFS1 in INS-1 832/13 cells increased the rate of ER-calcium depleted cells under ER stress or high-glucose conditions as expected (Figure 3H). Short hairpin RNA (shRNA)-mediated knockdown of WFS1 in HEK293 cells also increased the rate of ER calcium-depleted cells under normal and ER stress conditions (Figure 3I) and increased the cytosolic calcium concentrations (Figure 3J). This, in turn, increased expression levels of a proapoptotic molecule, CHOP (Figure 3K), leading to cell death (Figure 3L).

To further study the relationship between ER calcium levels and the disease causing mutations of the *WFS1* gene, we cloned different WFS1 mutants, R611H, P724L, G695V, and ins483fs/ter544 ,seen in patients with Wolfram syndrome (15) (Figure 3M). In addition to these autosomal recessive mutants, we also cloned an autosomal dominant mutant of WFS1, H313Y (33) (Figure 3M). Protein and mRNA expression levels of these WFS1 mutants are shown in Figure 3N. Although mRNA expression levels of these mutants were comparable, protein expression levels were slightly different between each mutant. Ectopic expression of WFS1 H313Y strongly activated the ER stress response element reporter (Figure 3O), raising the possibility that WFS1 H313Y causes ER stress through ER calcium depletion. To test this possibility, we measured the rates of ER calcium-depleted cells in HEK293 cells expressing WFS1 H313Y, wild-type WFS1, or an autosomal recessive WFS1 mutant, P724L. As we expected, the rate of ER calcium-depleted cells was increased by ectopic expression of WFS1 H313Y (Figure 3P). Collectively these results indicate that genetic factors involved in β-cell death can cause ER calcium depletion.

ER calcium depletion can lead to an increase in $[Ca^{2+}]_{cyt}$. It has been suggested that an increase in $[Ca^{2+}]_{cyt}$ activates a calcium-dependent proapoptotic protease, calpain-2, leading to β-cell death in type 2 diabetes (34–36). This prompted us to examine calpain-2 activation levels in stressed β-cells. To evaluate calpain-2 activation levels, we measured the cleavage of αII-spectrin, a substrate for calpain-2. Calpain-2 was activated in INS-1 832/13 cells treated with palmitate together with high glucose (Figure 4A), islets from db/db mice (Figure 4B), and human islets from persons with diabetes (Figure 4C), sug-

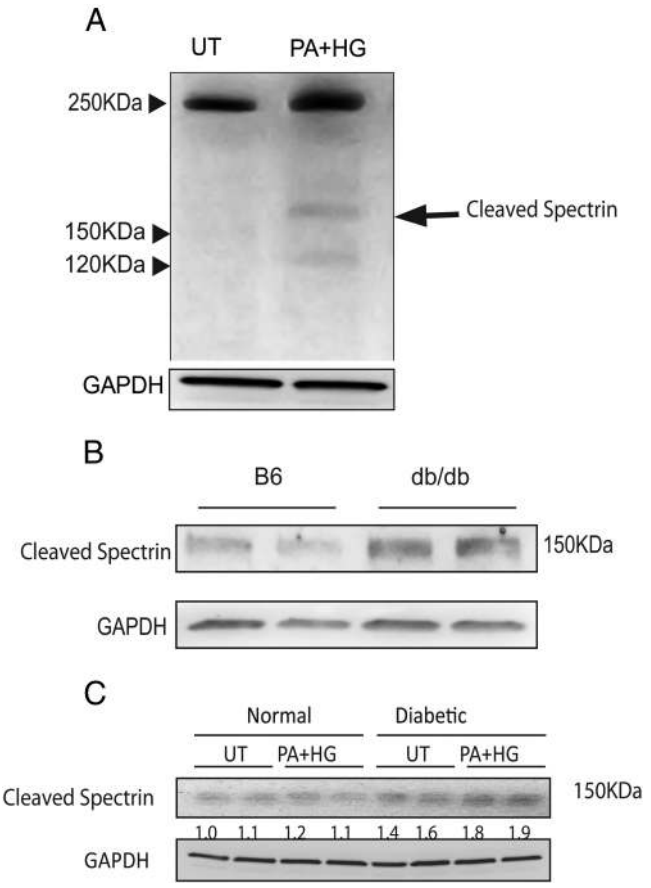

Figure 4. Calpain-2 activation in ER calcium-depleted β-cells. A, Cleaved spectrin levels in INS-1 832/13 cells were untreated or treated with 0.5 M palmitic acid (PA) together with 25 mM glucose (HG) for 24 hours. B, Cleaved spectrin levels in primary islets isolated from the age-matched B6 and db/db mice (male, 7 wk old). C, Cleaved spectrin level in human islets from nondiabetic and diabetic subjects. The islets were untreated or treated with palmitic acid (PA) together with 25 mM glucose (HG) for 24 hours.

Figure 3 (Continued). preproinsulin by a doxycycline inducible system. E, Rates of ER calcium-depleted INS-1 832/13 cells expressing D1ER calcium sensor and doxycycline-inducible A24D mutant insulin treated with or without doxycycline together with 1 mM TUDCA, 25 μM salburinal (SB), or 1 μM cycloheximide (CHX) for 24 hours (left panel). Caspase-3/7 activation levels in these cells are shown in the right panel. F, Rates of ER calcium-depleted INS-1 832/13 cells transfected with control scramble small interfering RNA (siRNA) or siRNA directed against WFS1 and then untreated or treated with 10 nM thapsigargin (TG) for 24 hours or 25 mM high glucose (HG; 25 mM) for 48 hours. G, Rates of ER calcium-depleted HEK293 cells transduced with lentivirus expressing control scramble shRNA or shRNA directed against WFS1 and then untreated or treated with 10 nM thapsigargin (TG) for 24 hours. H, Cytosolic calcium levels of HEK293 cells transduced with lentivirus expressing control scramble shRNA or shRNA directed against WFS1. Calcium levels were determined by Fluo-4 staining. I, Expression levels of CHOP mRNA in HEK293 cells transduced with lentivirus expressing control scramble shRNA or shRNA directed against WFS1 and then untreated or treated with 10 nM thapsigargin (TG) for 24 hours. J, Rates of cell death in HEK293 cells transduced with lentivirus expressing control scramble shRNA or shRNA directed against WFS1. K, Schematic representation of WFS1 protein showing mutations used in this study. L, Expression levels of ectopically expressed wild-type, H313Y, R611H, P724L, G695V, and Ter544 WFS1 mRNA (upper panel) and protein (middle panel) in HEK293 cells. GAPDH protein expression is shown in the bottom panel. M, Luciferase reporter assays in HEK293 cells transfected with the ER stress response element (ERSE) reporter together with control, wild-type WFS1, and mutant WFS1 expression plasmids. N, Rates of ER calcium-depleted INS1 832/13 cells transfected with control (pcDNA, empty expression plasmid), wild-type WFS1, H313Y WFS1, or P724L WFS1 expression plasmids and then treated with 10 nM thapsigargin for 24 hours. All values are means ± SEM (n = 3). *, $P < .05$; **, $P < .01$; ***, $P < .001$.

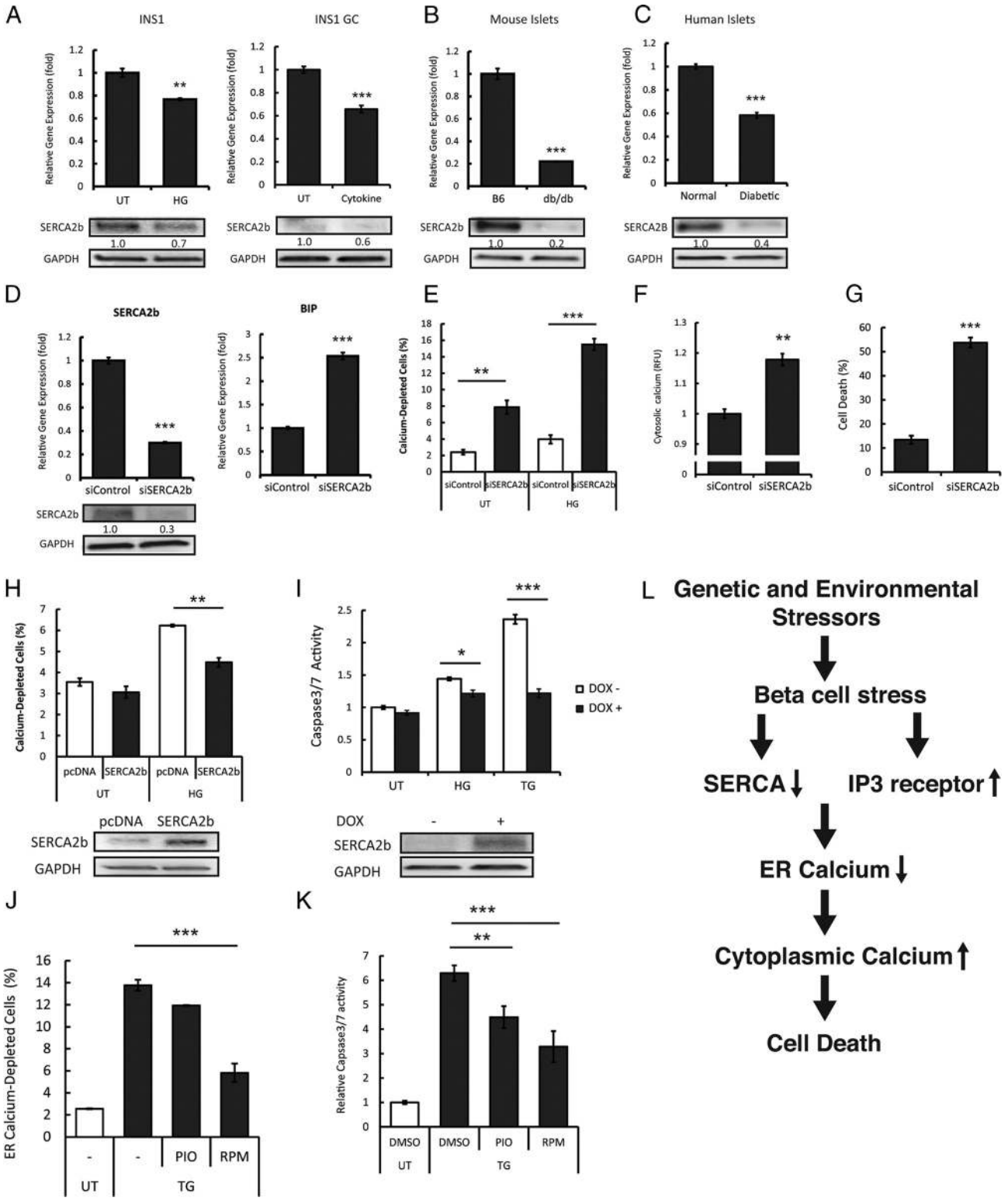

Figure 5. SERCA2b down-regulation and ER calcium depletion in disease states, and pharmacological intervention of ER calcium depletion. A, Expression levels of SERCA2b mRNA and protein in INS1 832/13 cells untreated (UT) or treated with high glucose (HG), and in INS1 GC cells untreated (UT) or treated with cytokines (100 ng/mL IL1-β, 100 ng/mL TNFα, and 100 ng/mL IFN-γ) for 48 hours. B, Expression levels of SERCA2b mRNA and protein in mouse primary islets isolated from control B6 or db/db mice (7 wk old, n = 6). C, Expression levels of SERCA2b mRNA and protein in human primary islets from normal (41 y old female with a BMI of 35.5 kg/m^2, no history of diabetes; glycosylated hemoglobin is 5.3) and diabetic (32 y old male, with a BMI of 28.2 kg/m^2; glycosylated hemoglobin is 6.9%; not on any medications) donors. D, Expression levels of SERCA2b and BiP in INS-1 832/13 cells transfected with control scramble small interfering RNA (siRNA) or siRNA directed against SERCA2b. E, Rates of ER calcium-depleted INS1 832/13 cells transfected with control scramble small interfering RNA (siRNA) or siRNA directed against SERCA2b and then treated with 11 mM (UT) or 25 mM glucose (HG) for 48 hours. F, Cytosolic calcium levels determined by Fluo-4 staining in INS-1 832/13

gesting that ER calcium depletion can lead to activation of calcium-dependent cell death pathways in the cytoplasm.

One of the genes required for ER calcium homeostasis is SERCA2b (5), raising the possibility that ER calcium depletion by environmental and genetic perturbants of β-cells might occur through down-regulation of SERCA2b. To test this idea, we first measured expression levels of SERCA2b in INS1 832/13 cells treated with chronic high-glucose (Figure 5A, left panel), INS1 GC cells treated with a cocktail of cytokines consisting of IL-1β, TNFα, and IFN-γ (Figure 5A, right panel), primary islets from db/db mice (Figure 5B), and human islets from persons with type 2 diabetes (Figure 5C). Expression levels of SERCA2b were decreased in these cells as compared with control cells. RNA interference-mediated knockdown of SERCA2b in INS1 832/13 cells significantly increased the expression of BiP, a well-known ER stress marker (Figure 5D), rate of ER calcium-depleted cells (Figure 5E), levels of resting $[Ca^{2+}]_{cyt}$ (Figure 5F), and rate of cell death (Figure 5G) under normal conditions. The depletion of ER calcium by SERCA2b knockdown was enhanced by chronic high-glucose treatment (Figure 5E). These results strongly suggest that calcium efflux from the ER in β-cells may occur through the down-regulation of SERCA2b, raising the possibility that SERCA2b overexpression might be beneficial for maintaining ER calcium homeostasis under various stress conditions. To test this idea, we overexpressed SERCA2b in β-cells and monitored ER calcium homeostasis and cell death. As we expected, ectopic expression of SERCA2b could prevent ER calcium depletion and cell death caused by chronic high glucose treatment in β-cells (Figure 5, H and I). SERCA2b overexpression also protected β-cells from ER stress-mediated cell death (Figure 5I).

The above results allowed us to draw the conclusion that β-cell perturbants induce calcium efflux from the ER, leading to cell death. This conclusion prompted us to ask whether chemical compounds blocking calcium efflux from the ER were able to prevent ER calcium depletion and β-cell death. Among the Food and Drug Administration-approved drugs we tested, pioglitazone and rapamycin could prevent ER calcium depletion mediated by thpasigargin (Figure 5J). The treatment of INS1 832/13 cells with pioglitazone and rapamycin could prevent ER stress-mediated cell death (Figure 5K). Collectively, these results indicate that blocking calcium efflux from the ER could prevent β-cell death.

Figure 5 (Continued). transfected with control scramble small interfering RNA (siRNA) or siRNA directed against Serca2b. G, Rates of cell death determined by propidium iodide staining in INS-1 832/13 cells transfected with control scramble small interfering RNA (siRNA) or siRNA directed against Serca2b for 72 hours. H, Rates of ER calcium-depleted INS-1 832/13 cells transfected with control empty expression plasmid (pcDNA) or expression plasmid for SERCA2b and then untreated in 11 mM glucose media (UT) or treated with 25 mM high glucose (HG). Protein expression levels of SERCA2b and GAPDH are shown in the lower panels. I, Apoptosis assays of INS-1 832/13 cells expressing doxycycline (DOX)-inducible SERCA2b treated (+) or untreated (−) with 2 μg/mL of DOX for 48 hours and then untreated in 11 mM glucose (UT), treated with 25 mM high glucose (HG), or treated with 10 nM thapsigargin for 24 hours. Apoptosis was monitored by caspase-3/7 activation levels. Protein expression levels of SERCA2b and GAPDH are shown in the lower panels. J and K, Rates of ER calcium-depleted (J) and apoptotic (K) INS-1 832/13 cells untreated (UT) or pretreated with 10uM pioglitazone (PIO) or 300 nM rapamycin (RPM) for the first 24 hours and then treated with 10 nM thapsigargin for the next 24 hours. Apoptosis was monitored by caspase-3/7 activation levels. All values are means ± SEM (n = 3). *, $P < .05$; **, $P < .01$; ***, $P < .001$. L, Scheme of cell death mediated by ER calcium depletion.

Discussion

It is well established that abnormal calcium levels in the cytosol are associated with disease states. However, the role of calcium depletion in the ER has not been extensively studied. The results presented here show that multiple conditions perturbing β-cell functions, including ER stress, oxidative stress, palmitate, and chronic high glucose, decrease ER calcium levels, leading to β-cell death. Genetic factors involved in β-cell death also cause ER calcium depletion (Figure 5L).

Previous studies have shown that SERCA2b expression is decreased in primary islets and β-cell lines under various disease states (5, 37). We have found that chronic high glucose decreases SERCA2b expression in β-cells. We have also shown that SERCA2b expression is decreased in islets from db/db mice and persons with type 2 diabetes, which was consistent with the previous report (37). Pioglitazone has been reported to increase SERCA2b expression levels in β-cells (37). We found that the pioglitazone can partially restore ER calcium levels under ER stress conditions. Our results combined with previous findings enable us to propose that molecular pathways regulating SERCA2b expression are attractive targets for preventing β-cell death in diabetes.

Opposing SERCA2b that pumps calcium into the ER, IP3 and ryanodine receptors mediate the release of calcium from the ER (1). Our results raise the possibility that dysregulation of IP_3 receptors and ryanodine receptors may precipitate β-cell death (Figure 5L). It has been shown that rapamycin inhibits IP3-mediated calcium release (38). Our results indicate that rapamycin can prevent ER calcium depletion and cell death mediated by ER stress. Modulation of IP3 receptor activity by rapamycin could be a novel therapeutic strategy for diseases related to ER dys-

function. Antiapoptotic Bcl-2 was reported to regulate IP3 receptor activity (39). However, the mechanism by which Bcl-2 regulates IP3 receptor activation is not clear. Our observations indicate that WFS1 regulates calcium efflux from the ER. Thus, it is possible that WFS1 or regulators of WFS1, inositol requiring-1, and PKR-like ER kinase may be involved in the regulation of IP3 receptor activation thorough the interaction with Bcl-2 (17, 40, 41).

Our results suggest that ER calcium depletion with subsequent increase in cytoplasmic calcium concentration can trigger calpain-2 activation, leading to β-cell death. It has been previously described that calpain 2 plays a key role in ER stress-mediated cell death through the activation of caspase-12 and c-Jun N-terminal kinase (35, 42). Calpain hyperactivation has been observed in β-cells of patients with type 2 diabetes and the brain samples of patients with Alzheimer's disease (34, 43). Thus, calpain-2 and its downstream signaling molecules, including caspase-12 and c-Jun N-terminal kinase, could be attractive targets for preventing β-cell death in diabetes and neuronal cell death in neurodegenerative diseases. Pharmacological modulation of ER calcium channels such the IP3 receptors and the ryanodine receptors or ER ATPase pumps, SERCAs, may have a beneficial effect in the survival of β-cells through the suppression of calpain-2. Our results suggest that rapamycin and pioglitazone can prevent calcium efflux from the ER and ER stress-mediated β-cell death by suppressing IP3 receptor and enhancing SERCA activation, respectively. Collectively our results indicate that identification of pathways and chemical compounds restoring ER calcium levels in disease states will lead to novel therapeutic modalities and pharmacological interventions for diabetes and other ER-related diseases including Wolfram syndrome.

Acknowledgments

We thank Karen Sargent, Cris Brown, and Mai Kanekura for technical assistance.

Address all correspondence and requests for reprints to: Fumihiko Urano, MD, PhD, Department of Medicine, Washington University School of Medicine, St Louis, MO 63110. E-mail: urano@dom.wustl.edu.

This work was supported by National Institutes of Health Grants DK067493, DK016746, P60DK020579, and UL1 TR000448; Juvenile Diabetes Research Foundation Grants 47-2012-760 and 17-2013-512), American Diabetes Association Grant 1-12-CT-61; the Ellie White Foundation for Rare Genetic Disorders; and the Jack and J. T. Snow Scientific Research Foundation (to F.U.).

Disclosure Summary: The authors have nothing to disclose.

References

1. **Berridge MJ, Bootman MD, Roderick HL.** Calcium signalling: dynamics, homeostasis and remodelling. *Nat Rev Mol Cell Biol*. 2003; 4(7):517–529.
2. **Mekahli D, Bultynck G, Parys JB, De Smedt H, Missiaen L. Endoplasmic-reticulum calcium depletion and disease.** *Cold Spring Harb Perspect Biol*. 2011;3(6).
3. **Berridge MJ, Lipp P, Bootman MD.** The versatility and universality of calcium signalling. *Nat Rev Mol Cell Biol*. 2000;1(1):11–21.
4. **Benkusky NA, Farrell EF, Valdivia HH.** Ryanodine receptor channelopathies. *Biochem Biophys Res Commun*. 2004;322(4):1280–1285.
5. **Cardozo AK, Ortis F, Storling J, et al.** Cytokines downregulate the sarcoendoplasmic reticulum pump Ca2+ ATPase 2b and deplete endoplasmic reticulum Ca2+, leading to induction of endoplasmic reticulum stress in pancreatic β-cells. *Diabetes*. 2005;54(2):452–461.
6. **Xu C, Bailly-Maitre B, Reed JC.** Endoplasmic reticulum stress: cell life and death decisions. *J Clin Invest*. 2005;115(10):2656–2664.
7. **Tersey SA, Nishiki Y, Templin AT, et al.** Islet β-cell endoplasmic reticulum stress precedes the onset of type 1 diabetes in the nonobese diabetic mouse model. *Diabetes*. 2012;61(4):818–827.
8. **O'Sullivan-Murphy B, Urano F.** ER stress as a trigger for β-cell dysfunction and autoimmunity in type 1 diabetes. *Diabetes*. 2012; 61(4):780–781.
9. **Oslowski CM, Hara T, O'Sullivan-Murphy B, et al.** Thioredoxin-interacting protein mediates ER stress-induced beta cell death through initiation of the inflammasome. *Cell Metab*. 2012;16(2): 265–273.
10. **Lerner AG, Upton JP, Praveen PV, et al.** IRE1α induces thioredoxin-interacting protein to activate the NLRP3 inflammasome and promote programmed cell death under irremediable ER stress. *Cell Metab*. 2012;16(2):250–264.
11. **Giacca A, Xiao C, Oprescu AI, Carpentier AC, Lewis GF.** Lipid-induced pancreatic Î²-cell dysfunction: focus on in vivo studies. *Am J Physiol Endocrinol Metab*. 300(2):E255–E262.
12. **Lai E, Bikopoulos G, Wheeler MB, Rozakis-Adcock M, Volchuk A.** Differential activation of ER stress and apoptosis in response to chronically elevated free fatty acids in pancreatic β-cells. *Am J Physiol Endocrinol Metab*. 2008;294(3):E540–E550.
13. **Gwiazda KS, Yang TL, Lin Y, Johnson JD.** Effects of palmitate on ER and cytosolic Ca2+ homeostasis in β-cells. *Am J Physiol Endocrinol Metab*. 2009;296(4):E690–E701.
14. **Barrett TG, Bundey SE, Macleod AF.** Neurodegeneration and diabetes: UK nationwide study of Wolfram (DIDMOAD) syndrome. *Lancet*. 1995;346(8988):1458–1463.
15. **Inoue H, Tanizawa Y, Wasson J, et al.** A gene encoding a transmembrane protein is mutated in patients with diabetes mellitus and optic atrophy (Wolfram syndrome). *Nat Genet*. 1998;20(2):143–148.
16. **Fonseca SG, Fukuma M, Lipson KL, et al.** WFS1 is a novel component of the unfolded protein response and maintains homeostasis of the endoplasmic reticulum in pancreatic β-cells. *J Biol Chem*. 2005; 280(47):39609–39615.
17. **Fonseca SG, Ishigaki S, Oslowski CM, et al.** Wolfram syndrome 1 gene negatively regulates ER stress signaling in rodent and human cells. *J Clin Invest*. 2010;120(3):744–755.
18. **Edghill EL, Flanagan SE, Patch A-M, et al.** Insulin mutation screening in 1,044 patients with diabetes: mutations in the INS gene are a common cause of neonatal diabetes but a rare cause of diabetes diagnosed in childhood or adulthood. *Diabetes*. 2008;57(4):1034–1042.
19. **Stoy J, Edghill EL, Flanagan SE, et al.** Insulin gene mutations as a cause of permanent neonatal diabetes. *PNAS*. 2007;104(38): 15040–15044.
20. **Liu M, Hodish I, Haataja L, et al.** Proinsulin misfolding and diabe-

tes: mutant INS gene-induced diabetes of youth. *Trends Endocrinol Metab*. 2010;21(11):652–659.
21. **Liu M, Haataja L, Wright J, et al.** Mutant INS-gene induced diabetes of youth: proinsulin cysteine residues impose dominant-negative inhibition on wild-type proinsulin transport. *PLoS One*. 2011; 5(10):e13333.
22. **Palmer AE, Tsien RY.** Measuring calcium signaling using genetically targetable fluorescent indicators. *Nat Protocols*. 2006;1(3):1057–1065.
23. **Robertson RP, Harmon J, Tanaka Y, Tran PO, Poitout V.** Glucose toxicity of the β-cell. In: LeRoith D, Taylor SI, Olefsky JM, eds. *Diabetes Mellitus*. Philadelphia: Lippincott Williams, Wilkins; 2004:129–139.
24. **Cnop M, Ladriere L, Hekerman P, et al.** Selective inhibition of eukaryotic translation initiation factor 2 α dephosphorylation potentiates fatty acid-induced endoplasmic reticulum stress and causes pancreatic β-cell dysfunction and apoptosis. *J Biol Chem*. 2007; 282(6):3989–3997.
25. **Cunha DA, Hekerman P, Ladriere L, et al.** Initiation and execution of lipotoxic ER stress in pancreatic β-cells. *J Cell Sci*. 2008;121(Pt 14):2308–2318.
26. **Cnop M.** Fatty acids and glucolipotoxicity in the pathogenesis of type 2 diabetes. *Biochem Soc Trans*. 2008;36(Pt 3):348–352.
27. **Cnop M, Igoillo-Esteve M, Cunha DA, Ladriere L, Eizirik DL.** An update on lipotoxic endoplasmic reticulum stress in pancreatic β-cells. *Biochem Soc Trans*. 2008;36(Pt 5):909–915.
28. **Weiss MA.** Proinsulin and the genetics of diabetes mellitus. *J Biol Chem*. 2009;284(29):19159–19163.
29. **Liu M, Lara-Lemus R, Shan SO, et al.** Impaired cleavage of preproinsulin signal peptide linked to autosomal-dominant diabetes. *Diabetes*. 2012;61(4):828–837.
30. **Fonseca SG, Urano F, Weir GC, Gromada J, Burcin M.** Wolfram syndrome 1 and adenylyl cyclase 8 interact at the plasma membrane to regulate insulin production and secretion. *Nat Cell Biol*. 2012; 14(10):1105–1112.
31. **Riggs AC, Bernal-Mizrachi E, Ohsugi M, et al.** Mice conditionally lacking the Wolfram gene in pancreatic islet β cells exhibit diabetes as a result of enhanced endoplasmic reticulum stress and apoptosis. *Diabetologia*. 2005;48(11):2313–2321.
32. **Ishihara H, Takeda S, Tamura A, et al.** Disruption of the WFS1 gene in mice causes progressive β-cell loss and impaired stimulus-secretion coupling in insulin secretion. *Hum Mol Genet*. 2004;13(11): 1159–1170.
33. **Hansen L, Eiberg H, Barrett T, et al.** Mutation analysis of the WFS1 gene in seven Danish Wolfram syndrome families; four new mutations identified. *Eur J Hum Genet*. 2005;13(12):1275–1284.
34. **Huang CJ, Gurlo T, Haataja L, et al.** Calcium-activated calpain-2 is a mediator of β cell dysfunction and apoptosis in type 2 diabetes. *J Biol Chem*. 2010;285(1):339–348.
35. **Tan Y, Dourdin N, Wu C, De Veyra T, Elce JS, Greer PA.** Ubiquitous calpains promote caspase-12 and JNK activation during endoplasmic reticulum stress-induced apoptosis. *J Biol Chem*. 2006;281(23): 16016–16024.
36. **Tan Y, Wu C, De Veyra T, Greer PA.** Ubiquitous calpains promote both apoptosis and survival signals in response to different cell death stimuli. *J Biol Chem*. 2006;281(26):17689–17698.
37. **Kono T, Ahn G, Moss DR, et al.** PPAR-γ activation restores pancreatic islet SERCA2 levels and prevents β-cell dysfunction under conditions of hyperglycemic and cytokine stress. *Mol Endocrinol*. 2012;26(2):257–271.
38. **MacMillan D, McCarron JG.** Regulation by FK506 and rapamycin of Ca2+ release from the sarcoplasmic reticulum in vascular smooth muscle: the role of FK506 binding proteins and mTOR. *Br J Pharmacol*. 2009;158(4):1112–1120.
39. **Oakes SA, Scorrano L, Opferman JT, et al.** Proapoptotic BAX and BAK regulate the type 1 inositol trisphosphate receptor and calcium leak from the endoplasmic reticulum. *Proc Natl Acad Sci USA*. 2005;102(1):105–110.
40. **Fonseca SG, Gromada J, Urano F.** Endoplasmic reticulum stress and pancreatic β-cell death. *Trends Endocrinol Metab*. 2011;22(7): 266–274.
41. **Oslowski CM, Urano F.** The binary switch that controls the life and death decisions of ER stressed beta cells. *Curr Opin Cell Biol*. 2011; 23(2):207–215.
42. **Nakagawa T, Yuan J.** Cross-talk between two cysteine protease families. Activation of caspase-12 by calpain in apoptosis. *J Cell Biol*. 2000;150(4):887–894.
43. **Saito K, Elce JS, Hamos JE, Nixon RA.** Widespread activation of calcium-activated neutral proteinase (calpain) in the brain in Alzheimer disease: a potential molecular basis for neuronal degeneration. *Proc Natl Acad Sci USA*. 1993;90(7):2628–2632.